Free Radical Research, June 2010; 44(6): 624–634

The neem limonoids azadirachtin and nimbolide induce cell cycle arrest and mitochondria-mediated apoptosis in human cervical cancer (HeLa) cells

R. VIDYA PRIYADARSINI[1], R. SENTHIL MURUGAN[1], P. SRIPRIYA[2], D. KARUNAGARAN[2] & S. NAGINI[1]

[1]*Department of Biochemistry and Biotechnology, Faculty of Science, Annamalai University, Annamalainagar-608 002, Tamil Nadu, India, and* [2]*Department of Biotechnology, Indian Institute of Technology, Madras, Chennai-600 036, Tamil Nadu, India*

(Received date 13 November 2009; In revised form date 19 January 2010)

Abstract

Limonoids from the neem tree (*Azadirachta indica*) have attracted considerable research attention in recent years owing to their potent antioxidant and anti-proliferative effects. The present study was designed to investigate the cellular and molecular mechanisms by which azadirachtin and nimbolide exert cytotoxic effects in the human cervical cancer (HeLa) cell line. Both azadirachtin and nimbolide significantly suppressed the viability of HeLa cells in a dose-dependent manner by inducing cell cycle arrest at G0/G1 phase accompanied by p53-dependent p21 accumulation and down-regulation of the cell cycle regulatory proteins cyclin B, cyclin D1 and PCNA. Characteristic changes in nuclear morphology, presence of a subdiploid peak and annexin-V staining pointed to apoptosis as the mode of cell death. Increased generation of reactive oxygen species with decline in the mitochondrial transmembrane potential and release of cytochrome *c* confirmed that the neem limonoids transduced the apoptotic signal via the mitochondrial pathway. Altered expression of the Bcl-2 family of proteins, inhibition of NF-κB activation and over-expression of caspases and survivin provide compelling evidence that azadirachtin and nimbolide induce a shift of balance toward a pro-apoptotic phenotype. Antioxidants such as azadirachtin and nimbolide that can simultaneously arrest the cell cycle and target multiple molecules involved in mitochondrial apoptosis offer immense potential as anti-cancer therapeutic drugs.

Key words: *Antioxidant, apoptosis, azadirachtin, cell cycle, neem, nimbolide*

Introduction

Tumour resistance to apoptotic cell death, an important hallmark of cancer, contributes to increased survival of cells that have acquired oncogenic mutations, eventually leading to uncontrolled cell proliferation, invasion, metastasis, angiogenesis and chemoresistance [1]. Apoptosis occurs in a highly coordinated manner with characteristic features such as nuclear and cytoplasmic condensation, inter-nucleosomal cleavage, phosphatidylserine externalization, formation of membrane-bound apoptotic bodies and phagocytosis of the affected cell [2,3]. Two major canonical signalling pathways that lead to apoptotic cell death have been recognized in mammals—the *extrinsic or death receptor pathway* mainly implicated in the maintenance of tissue homeostasis and the *intrinsic or mitochondrial pathway* that occurs in response to various extracellular cues and internal insults such as DNA damage [1,4,5]. Both the pathways converge at the activation of the enzymatic caspase cascade, culminating in apoptotic cell death [6].

Cancer cells evade apoptosis by downregulation of death receptors, altered expression of the Bcl-2 family proteins that control mitochondrial release of apoptogenic molecules such as cytochrome *c*, constitutive activation of nuclear factor-κB (NF-κB), a pro-survival and anti-apoptotic transcription factor

Correspondence: Dr. S. Nagini, Professor, Department of Biochemistry and Biotechnology, Faculty of Science, Annamalai University, Annamalainagar-608 002, Tamil Nadu, India. Tel: +91-4144-239842. Fax: +91-4144-238145/238080. Email: s_nagini@yahoo.com; snlabau@gmail.com

ISSN 1071-5762 print/ISSN 1029-2470 online © 2010 Informa UK Ltd. (Informa Healthcare, Taylor & Francis AS)
DOI: 10.3109/10715761003692503

and over-expression of inhibitors of apoptosis proteins (IAPs) [1,7–9]. Identification of agents that target these molecules that play a crucial role in the regulation of apoptosis has evolved as a new paradigm in anti-cancer drug development. In particular, phytochemicals from medicinal plants have received growing attention in recent years as potential chemopreventive and chemotherapeutic agents owing to their apoptosis-inducing effects [10].

Of late, limonoids, modified triterpenes found abundantly in various parts of the neem tree (*Azadirachta indica* A. Juss), have attracted considerable research attention as potential anti-neoplastic agents [11]. Azadirachtin, isolated from seed kernels, and nimbolide present in leaves and flowers, are the two most important neem limonoids that exhibit potent cytotoxic effects against a panel of human cancer cell lines [12–14]. Figure 1 presents the chemical structures of nimbolide and azadirachtin. Recently, we reported the chemopreventive potential of azadirachtin and nimbolide in an animal model of oral oncogenesis based on their ability to modulate host antioxidant defences, cell proliferation, apoptosis evasion, invasion, metastasis and angiogenesis [15,16].

In the present study, we examined the cellular and molecular mechanisms by which azadirachtin and nimbolide exert cytotoxic effects in the human cervical cancer (HeLa) cell line. Both azadirachtin and nimbolide induced characteristic changes in nuclear morphology, presence of a sub-diploid peak and annexin-V staining, indicating apoptosis as the mode of cell death. Increased ROS generation with decline in the mitochondrial transmembrane potential, release of cytochrome *c* and up-regulation of pro-apoptotic members of the Bcl-2 family, as well as caspases and survivin, implicated the mitochondrial pathway of apoptosis. In addition, both the neem limonoids inhibited NF-κB activation and modulated the expression of cell cycle associated proteins.

Materials and methods

Chemicals

Azadirachtin and nimbolide of purity≥97% were purchased from SPIC Science Foundation (Tuticorin, India). Stock solutions of azadirachtin and nimbolide were prepared by dissolving in phosphate buffered saline (PBS) containing 0.5% DMSO. The stock solutions were then diluted with Dulbecco's modified Eagles medium (DMEM) prior to use to obtain the desired concentration. Acridine orange, 4,6-diamidino-2-phenylindol (DAPI), 2',7'-dichlorofluorescein diacetate (DCFH-DA), ethidium bromide, glutathione (GSH), JC-1 iodide and propidium iodide were purchased from Sigma Chemical Company (St. Louis, MO).

Cell culture and maintenance

HeLa cells were procured from the National Centre for Cell Science (Pune, India). The cells were grown in DMEM (GIBCO BRL, Grand Island, NY) containing 10% FBS (Sigma) and antibiotics (100 U/ml of penicillin and 100 μg/ml of streptomycin). Cells were maintained as monolayer cultures in a humidified atmosphere of 5% CO_2 at 37°C.

Determination of cell viability

Cell viability was determined based on the trypan blue exclusion method. Briefly, HeLa cells were plated at a density of 1×10^5 cells/ml into 24-well plates. After overnight growth, cells were pre-treated with a series of concentrations of azadirachtin (0–200 μM) and nimbolide (0–10 μM), respectively, for 24 h. Subsequently, the medium was removed from the wells by aspiration and the cells were washed with PBS. Trypsin-EDTA was then added to the wells in order to detach cells from the substratum. Finally the cells were resuspended in fresh medium and counted under the microscope using trypan blue as a marker of cell viability. Relative cell viability (in percentage) was expressed as (number of viable treated cells/number of viable control cells)×100. All doses were tested in triplicate and the experiment was repeated at least three times.

Assessment of nuclear morphology

Characteristic apoptotic morphological changes were assessed by fluorescent microscopy using acridine

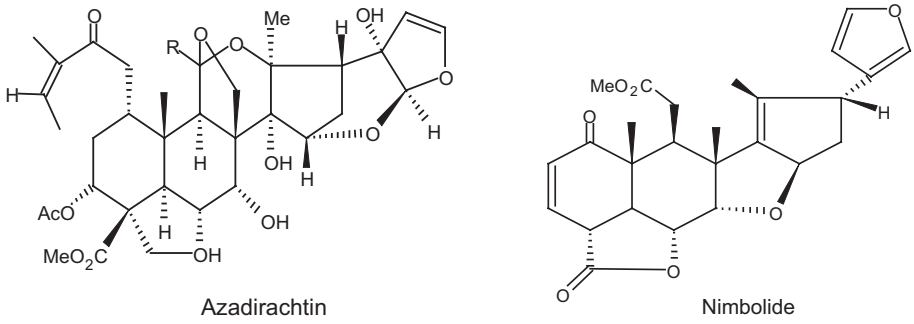

Figure 1. Chemical structures of azadirachtin and nimbolide.

orange/ethidium bromide (AO/EB) and DAPI staining. HeLa cells grown in 12-well plate at seeding densities of 2×10^5 cells were treated with azadirachtin (135 μM) and nimbolide (5 μM) for 24 h. After washing once with phosphate buffered saline (PBS), the cells were incubated with 100 μl of a mixture (1:1) of AO/EB (4 μg/ml) solutions. For DAPI staining, cells were fixed in ice-cold methanol (–20°C) for 15 min and stained with DNA-specific fluorochrome DAPI (1 μg/ml) for 30 min in the dark. The cells were immediately washed with DMEM, viewed and photographed using Nikon inverted fluorescent microscope (TE-Eclipse 300).

Cell cycle analysis

Cell cycle distribution and measurement of the percentage of apoptotic cells were performed by flow cytometry. HeLa cells were plated in six well plates at a density of 5×10^6 cells/well. After 24 h of treatment, cells were harvested by trypsinization and washed twice with PBS. Cells were then gently fixed with 70% ice cold ethanol at –20°C for 1 h and resuspended in PBS containing 0.5 μg/ml RNase and incubated at 37°C for 30 min. Following this, cells were stained with 1 ml of 50 μg/ml propidium iodide for 10 min and the DNA content was analysed on a flow cytometer (FACSort, Becton Dickinson, San Jone, USA).

Annexin V-PI test

To quantify limonoid-induced apoptotic cell death, we used the dual staining abilities of the probes annexin V and propidium iodide. Briefly, after treatment, adhering cells were harvested by trypsinization and washed twice with PBS. Cells were then resuspended in binding buffer and stained with annexin V-FITC and PI according to the instructions of the manufacturer (Annexin V-FITC-PI apoptosis detection kit, Sigma). The cells were incubated in the dark for 10 min and analysed by a flow cytometer using excitation/emission wavelengths of 488/525 nm and 488/675 nm for annexin V and PI, respectively.

Determination of ROS generation

Intracellular ROS generation was monitored spectrofluorimetrically (Perkin Elmer, Germany) using the oxidation-sensitive fluorescent probe DCFH-DA. Briefly, after 24 h of treatment, cells were harvested and suspended in 0.5 ml PBS containing 10 μM DCFH-DA for 15 min at 37°C in the dark. DCFH-DA was taken up by cells and deacetylated by cellular esterase to form a non-fluorescent product DCFH, which is converted to a green fluorescent product DCF by intracellular ROS produced by treated HeLa cells. The intensity of DCF fluorescence was measured at 530 nm after excitation at 488 nm [17]. ROS levels were expressed as percentage over control.

Analysis of mitochondrial transmembrane potential

The changes in the mitochondrial transmembrane potential ($\Delta\psi M$) were determined using JC-1, a fluorescent carbocyanine dye, which accumulates in the mitochondrial membrane as a monomer or dimer depending on mitochondrial membrane potential [18]. Briefly, cells were plated at a seeding density of 2×10^5 cells/well in a 12-well plate. After 24 h of drug treatment, cells were incubated with 5 μM JC-1 for 30 min at room temperature in the dark. The presence of JC-1 monomers or dimers was examined under a fluorescent microscope using filter pairs of 530 nm/590 nm (dimers) and 485 nm/538 nm (monomers).

RNA isolation and cDNA synthesis

Following treatment, HeLa cells grown in 60 mm petri dishes were washed with ice-cold PBS and 1 ml of trizol was added and flushed gently to disrupt the cells. The lysates were collected and mixed with 300 μl of chloroform by inversion. The tubes were then centrifuged at 10 000 rpm for 15 min at 4°C. The aqueous phases from the tubes were collected and the RNA was precipitated using 700 μl of isopropanol and centrifuged at 10 000 rpm for 10 min at 4°C. The pellets were washed twice with 70% ethanol and air-dried for ~ 20–40 min. The pellets were resuspended in 100 μl of DEPC-treated water and the RNA concentration was determined from the optical density at a wavelength of 260 nm (by using an OD_{260} unit equivalent to 40 μg/ml of RNA).

Isolated total RNA (1 μg) was reverse-transcribed to cDNA in a reaction mixture containing 4 μl of 5X reaction buffer, 2 μl of dNTPs mixture (10 mM), 20 units of RNase inhibitor, 200 units of avian-myeloblastosis virus (AMV) reverse transcriptase and 0.5 μg of oligo(dT) primer (Promega, WI) in a total volume of 20 μl. The reaction mixture was incubated at 42°C for 60 min and the reaction terminated by heating at 70°C for 10 min. The resultant cDNA was stored at –80°C until further use.

PCR amplification

All oligonucleotide primers were purchased from Sigma Genosys (India). Details about the primers are given in Table I. The PCR amplification reaction mixture (in a final volume of 25 μl) contained 1 μl of cDNA, 0.5 μl of forward primer, 0.5 μl of reverse primer and 10 μl of Hot Master Mix (2.5X) (Eppendorf, Hamburg, Germany). The PCR was carried out in a thermal cycler (Eppendorf). Negative controls without cDNA were also performed. Amplification

Table I. Oligonucleotide primers for RT-PCR analysis

Gene product	Primer sequences	Fragment size (bp)
Bad	Sense 5'-CCCAGAGTTTGAGCCGAGTG-3'	317
	Antisense 5'-GCTGTGCTGCCCAGAGGTT-3'	
Bax	Sense 5'-ACCAAG CTGAGCGA GTGTC-3'	293
	Antisense 5'-ACAAAGATGGTCACGGTCTGCC-3'	
Bcl-2	Sense 5'-ACCAAG CTGAGCGA GTGTC-3'	415
	Antisense 5'-ACAAAGATGGTCACGGTCTGCC-3'	
Bcl-xL	Sense 5'-GAGGCAGGCGACGAGTTT-3'	320
	Antisense 5'-GACGGAGGATGTGGTGGA-3'	
Bid	Sense 5'-ACAAGGCCATGCTGATAATGACAAT-3'	302
	Antisense 5'-CTGCGTTCAGCTTGAGTGTATCTG-3'	
Caspase -3	Sense 5'-GACAACAACGAAACCTCCGT-3'	382
	Antisense 5'-GACTTCGTATTTCAGGGCCA-3'	
Caspase -9	Sense 5'-TGTGGTGGTCATCCTCTCTCA-3'	282
	Antisense 5'-GTCACTGGGGGTAGGCAAACT-3'	
Cytochrome *c*	Sense 5'-GGAGGCAAGCATAAGACTGG-3'	267
	Antisense 5'-GTCTGCCCTTTCTCCCTTCT-3'	
p21	Sense 5'-CTCAGAGGAGGCGCCATG-3'	517
	Antisense 5'-GGGCGGATTAGGGCTTCC-3'	
p53	Sense 5'-GTTTCCGTCTGGGCTTCTTG-3'	473
	Antisense 5'-CCTGGGCATCCTTGAGTTCC-3'	
PCNA	Sense 5'-GCCCTCAAAGACCTCATCAA-3'	472
	Antisense 5'-GCTCCCCACTCGCAGAAAAC-3'	
β-Actin	Sense 5'-AACCGCGAGAAGATGACCCAGATCATGTTT-3'	350
	Antisense 5'-AGCAGCCGTGGCCATCTCTTGCTCGAAGTC-3'	

products were analysed by electrophoresis in a 2% agarose gel containing ethidium bromide with 100bp DNA ladder. The PCR products were visualized as bands with a UV-transilluminator and photographs were taken using gel documentation system (GelDoc-Mega^{TM}, UK).

Western blot analysis

Following treatment, cells were washed three times with PBS and lysed in a RIPA lysis buffer (50 mM Tris-HCl (pH 7.4), 1% Nonidet P-40, 40 mM NaF, 10 mM NaCl, 10 mM Na_3VO_4, 1 mM phenylmethanesulphonyl fluoride (PMSF), 10 mM dithiothreitol (DTT)). The cell lysates were centrifuged at 14 000 rpm for 15 min. For the isolation of mitochondrial fraction, cells were washed with PBS and scraped in homogenizing buffer (10 mM HEPES (pH 7.9), 10 mM KCl, 0.1 mM EDTA, 0.1 mM EGTA, 1 mM DTT, 0.5 mM PMSF, 10 mM sucrose). The homogenate was centrifuged at 1000 g for 5 min to remove the nuclear and unbroken cells. The supernatant was centrifuged at 23 100 g for 30 min at 4°C and the resulting pellet containing mitochondria was resuspended in lysis buffer (150 mM NaCl, 0.5% Triton X-100, 50 mM Tris, 20 mM EGTA, 1 mM DTT, 1 mM sodium orthovanadate and protease inhibitor cocktail). Total protein was determined by the method of Bradford [19].

Proteins separated by SDS-PAGE were electrophoretically transferred to polyvinylidene difluoride membranes. The membranes were incubated in 1X PBS containing 5% non-fat dry milk for 2 h to block non-specific binding sites. The blots were incubated with primary antibodies (diluted according to the manufacturer's instructions) for 30–45 min at room temperature. After washing, the blots were incubated with 1:1000 dilutions of horseradish peroxidase-conjugated secondary antibodies (Santa Cruz Biotechnology, CA) for 45 min at room temperature. After extensive washes with high and low salt buffers, the immunoreactive proteins were visualized using enhanced chemiluminescence (ECL) detection reagents (Sigma). Densitometry was performed on IISP flat bed scanner and quantitated with Total Lab 1.11 software.

Statistical analysis

Cytotoxicity data are presented as mean percentages of control ± SD and linear regression analysis was used to calculate IC_{50} values. The data for apoptotic cell death were analysed by Student's *t*- test. Densitometric analysis data for RT-PCR and western blot were analysed using analysis of variance (ANOVA) and the group means were compared by the least significant difference test (LSD). The results were considered statistically significant if $p < 0.05$.

Results

Azadirachtin and nimbolide cause dose-dependent reduction in survival of HeLa cells

We first tested the cytotoxic effects of different concentrations of azadirachtin (0–200 μM) and nimbolide (0–10 μM) on the growth of HeLa cells. Incubation of HeLa cells for 24 h with azadirachtin and nimbolide caused dose-dependent inhibition of

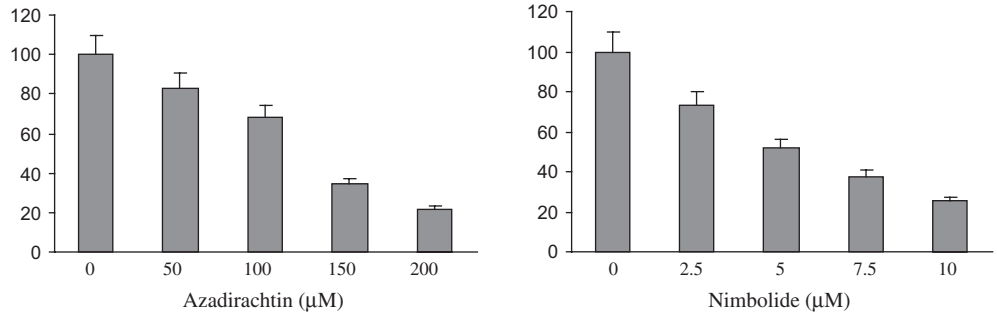

Figure 2. Effects of azadirachtin and nimbolide on HeLa cell viability. Cell viability was determined by trypan blue assay as described. IC_{50} concentration of azadirachtin = 135 μM; and nimbolide = 5 μM. Data are represented as mean ± SD of three independent determinations, each performed in triplicate.

growth of cells, with IC_{50} values of 135 and 5 μM, respectively (Figure 2).

Azadirachtin and nimbolide induced apoptosis in HeLa cells

To characterize whether the decrease in cell viability was caused by apoptosis, we observed changes in the nuclear morphology of HeLa cells using the fluorescent DNA binding dyes AO/EB and DAPI. As shown in Figure 3, treatment of HeLa cells for 24 h with IC_{50} concentrations of azadirachtin and nimbolide resulted in significant chromosomal condensation and morphological changes, indicating that the cytotoxic action of azadirachtin and nimbolide was due to its ability to induce apoptosis.

Apoptotic cell death is characterized by specific changes in the presence of sub-diploid peak [20]. To investigate the induction of a subG1-cell population, the DNA content of HeLa cells treated with azadirachtin and nimbolide was analysed by flow cytometry. Treatment of HeLa cells with IC_{50} concentrations of azadirachtin and nimbolide resulted in an increase in the proportion of cells with reduced DNA content compared to control. The percentage of apoptotic cells was 34% and 45% in azadirachtin and nimbolide treated cells, respectively (Figure 4). To further confirm apoptosis induced by azadirachtin and nimbolide, HeLa cells were stained with annexin V-FITC and PI and subsequently analysed by flow cytometry. The annexin V assay evaluated phospholipid turnover from the inner to the outer lipid layer of the plasma membrane, an event typically associated with apoptosis. As shown in Figure 5, the proportion of annexin V stained cells increased from 0.13% (control) to 9.5% and 21.3% in azadirachtin and nimbolide treated cells, respectively.

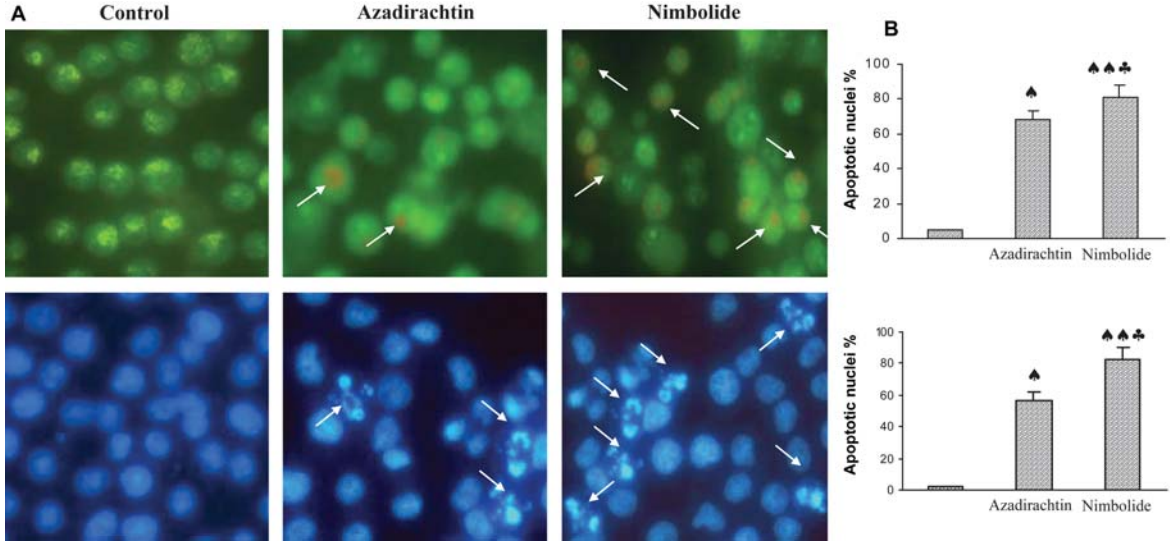

Figure 3. Morphological changes and the number of apoptotic nuclei formed after treatment with IC_{50} concentrations of azadirachtin and nimbolide for 24 h. (A) AO/EB staining and DAPI staining. (B) Error bar represents SD between counts of three independent experiments. ♠- significantly different from control ($p<0.001$) by Student's t-test. ♠♠- significantly different from control ($p<0.001$) ♣- significantly different from azadirachtin ($p<0.05$). Apoptotic cells are shown as white arrowheads.

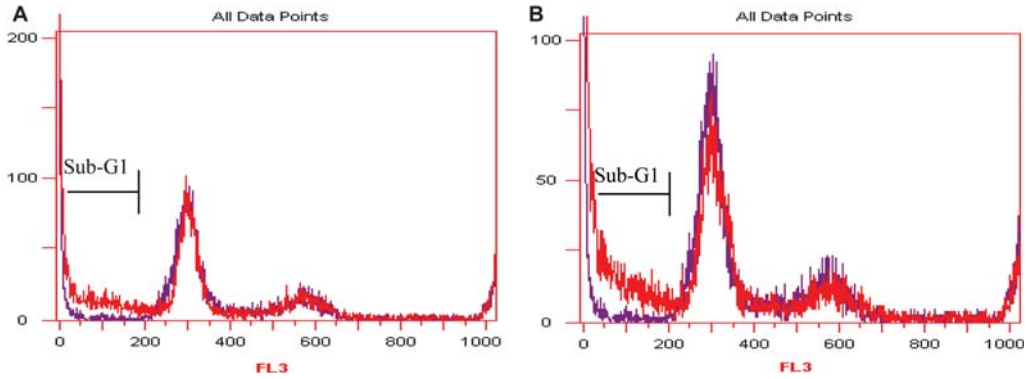

Figure 4. DNA content of HeLa cells treated with IC_{50} concentrations of azadirachtin (A) and nimbolide (B) detected by flow cytometry. Sub G1 cells represent apoptotic cells with a lower DNA content. The data presented are representative of three independent experiments.

Involvement of ROS production and mitochondrial dysfunction in azadirachtin- and nimbolide-induced apoptosis

There is accumulating evidence to indicate that ROS plays an important role in apoptosis induction [21]. We analysed ROS generation using the fluorescent probe DCFH-DA. Treatment with azadirachtin (135 μM) and nimbolide (5 μM) for 24 h significantly increased ROS generation in HeLa cells compared to control (Figure 6A). Furthermore, addition of GSH decreased the cytotoxic effects of azadirachtin and nimbolide (Figure 6B). These results suggest the involvement of ROS in the cytotoxic effects of azadirachtin and nimbolide on HeLa cells.

We next evaluated the effects of azadirachtin and nimbolide on ΔψM using JC-1. JC-1 has the unique property of forming red fluorescent aggregates spontaneously under high mitochondrial potential, whereas the monomeric form is prevalent in cells with low ΔψM and fluoresces in green. Treatment of HeLa cells with azadirachtin (135 μM) and nimbolide (5 μM) for 24 h resulted in collapse of the mitochondrial membrane potential, as revealed by a change in fluorescence from red to green, compared to control (Figure 7).

Azadirachtin- and nimbolide-induced expression of cell cycle arrest and pro-apoptotic proteins

To investigate the effects of azadirachtin (135 μM) and nimbolide (5 μM) on the expression of markers associated with cell survival, proliferation and apoptosis, we analysed the mRNA and protein expression of p53, p21, cyclin D1, PCNA, NF-κB family members (p50, p65, IκB, p-IκB-*α* and IKK*β*), survivin, Bcl-2 family members (Bcl-2, Bcl-xL, Mcl-1, Bid, Bad and Bax), cytochrome *c* (cytosolic and mitochondrial), Apaf-1, caspases (caspase –2L, –6, –8, –9 and –3) and PARP cleavage by RT-PCR and western blot analyses using *β*-actin as internal control (Figures 8 and 9). Quantification of each band by densitometric analysis revealed significant increase in the expression of p53, p21, IκB, Bid, Bad, Bax, cytosolic cytochrome C, Apaf-1, caspase –2L, –6, –8, –9 and –3 and PARP cleavage with decrease in the expression of cyclin D1, PCNA, NF-κB, p-IκB-*α*, IKK*β*, survivin, Bcl-2, Bcl-xL, Mcl-1 and mitochondrial cytochrome *c* in HeLa cells treated with azadirachtin and nimbolide compared to untreated control. *β*-actin was not detected in the mitochondrial fractions, indicating that there was no mitochondrial contamination from the cytosolic fraction.

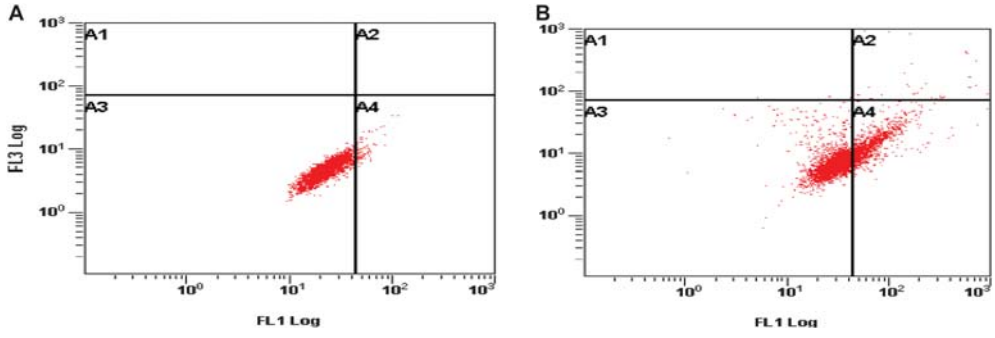

Figure 5. Scatter plots of Annexin V-FITC/PI stained HeLa cells treated with IC_{50} concentrations of azadirachtin (A) and nimbolide (B) under four situations in a quadrant analysis. (A1) Necrotic or dead cells, (A2) late apoptotic or dead cells, (A3) living cells, (A4) early apoptotic cells. The data presented are representative of three independent experiments.

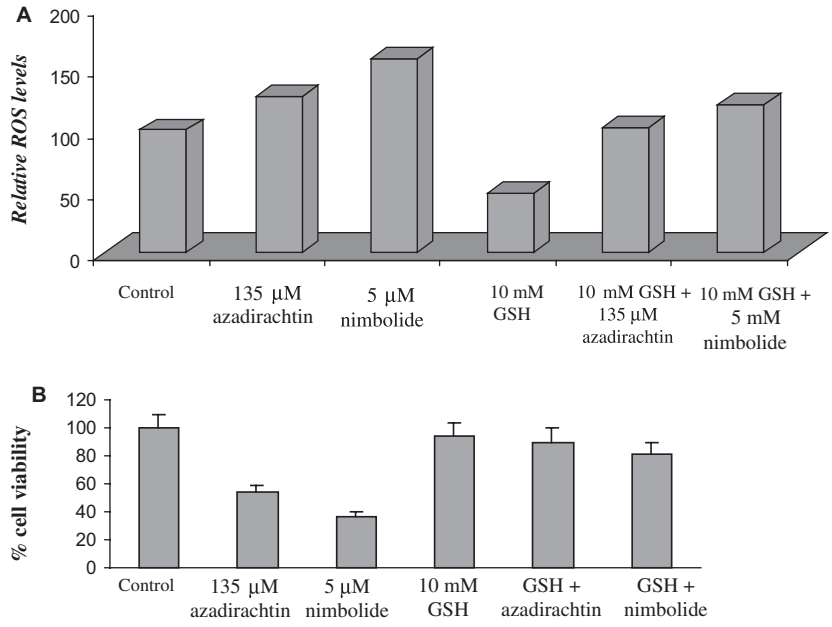

Figure 6. (A) Effect of azadirachtin and nimbolide on ROS generation. HeLa cells were treated with 135 and 5 μM azadirachtin and nimbolide in the presence or absence of GSH and the DCF fluorescence was measured by spectrofluorimetry. (B) Effect of GSH on cytotoxicity of HeLa cells by azadirachtin and nimbolide.

Discussion

The cytotoxic and anti-proliferative effects of azadirachtin and nimbolide have been demonstrated in a panel of cancer cell lines. Cohen et al. [13] found nimbolide to be a more potent anti-proliferative agent relative to azadirachtin based on the cytotoxic effects against NIE-155, 143.BK.TK and RAW 264.7 cancer cell lines. In addition, a vast panel of leukaemic and melanoma cell lines as well as human choriocarcinoma (BeWo) cells displayed sensitivity to the cytotoxicity of nimbolide [14,22,23]. The dose-dependent suppression of viability of HeLa cells by azadirachtin and nimbolide seen in the present study underscores the growth inhibitory potential of these neem limonoids.

Analysis of cell cycle distribution revealed a greater proportion of cells in sub G0/G1 and a lesser proportion in S and G2/M phase. Notably, cell cycle arrest at G0/G1 phase was accompanied by p53-dependent p21 accumulation and down-regulation of the cell cycle regulatory proteins cyclin B, cyclin D1 and PCNA. Consistent with our findings, Roy et al. [14] demonstrated a remarkable increase in the number of cells in subG1 fraction with a reciprocal decrease of cells in all other phases in U937 cells exposed to nimbolide. In another study, HT-29 cells exposed to nimbolide showed G2/M phase arrest, up-regulation of p21 and chk2 with down-regulation of cyclin A, cyclin E, cdk2 and Rad17 [22].

In addition to cell cycle arrest, azadirachtin and nimbolide induced morphological features characteristic of apoptotic cell death such as detachment of cells from the substratum, an increase in the number of sub-diploid cells, chromatin condensation and appearance of annexin-V-positive cells. Elucidation of the molecular mechanism underlying apoptosis by these neem limonoids revealed ROS generation,

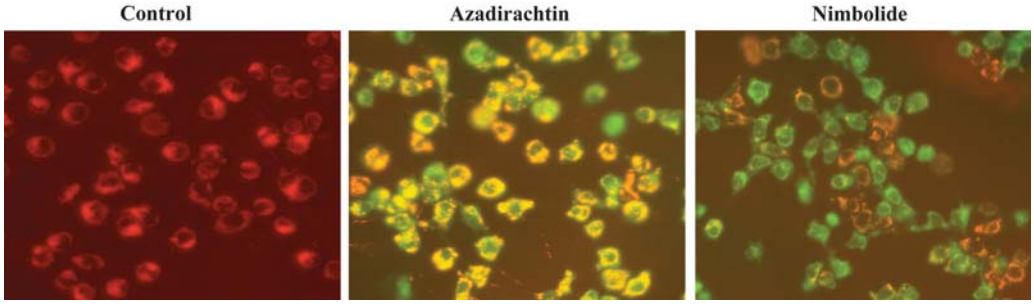

Figure 7. Fluorescent microscopy images of control cells and cells treated with IC_{50} concentrations of azadirachtin and nimbolide. Yellow-orange fluorescence is visible in cell areas with high mitochondrial membrane potential, while green fluorescence of JC-1 monomer is present in cell areas with low mitochondrial membrane potential.

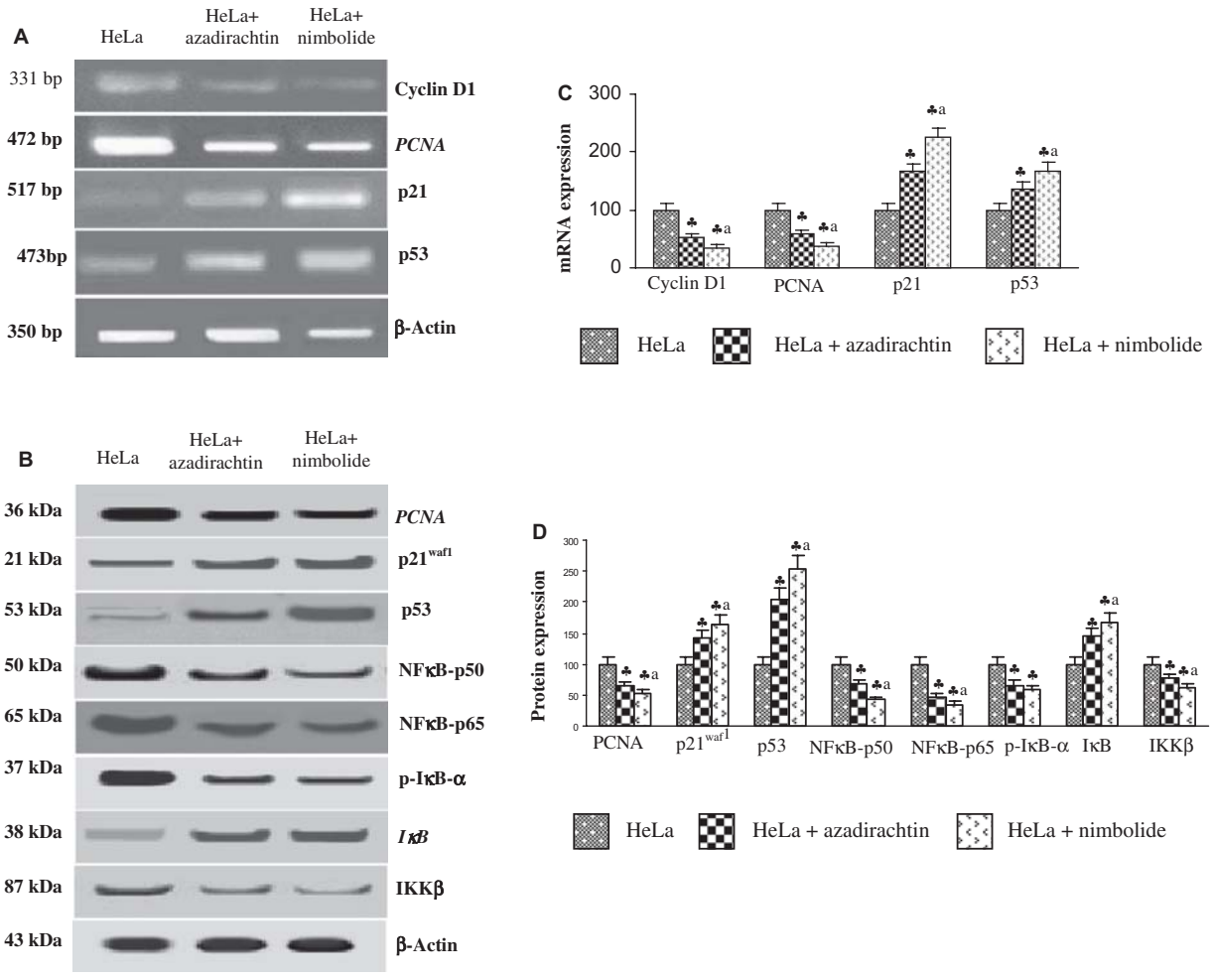

Figure 8. Effects of azadirachtin (135μM) and nimbolide (5μM) on markers of cell proliferation and survival in HeLa cells. (A) Representative RT-PCR analyses. β-Actin was used as an internal control. (B) Representative immunoblots. Protein samples (50 μg/lane) resolved on SDS PAGE were probed with corresponding antibodies. β-Actin was used as loading control. (C, D) Densitometric analysis. ♣Significantly different from HeLa ($p<0.01$) ANOVA followed by LSD. 'a' Significantly different from HeLa$^+$ Azadirachtin ($p<0.05$).

decline in the mitochondrial transmembrane potential with consequent release of cytochrome *c* and increased expression of Apaf-1, as well as initiator and effector caspases culminating in PARP cleavage. Addition of the antioxidant glutathione blocked ROS generation and the cytotoxic effects of azadirachtin and nimbolide confirming ROS involvement. The pro-oxidant behaviour of these neem limonoids in HeLa cells is similar to that exhibited by several antioxidant phytochemicals such as curcumin, resveratrol and tea polyphenols in cancer cell lines and may be attributed to the cellular redox status, free radical source, partial pressure of oxygen and ability to participate in a Fenton type chemical reaction [24–27].

Permeabilization of the outer mitochondrial membrane, a critical step in stimulating cell death, is regulated by the opposing actions of pro- and anti-apoptotic members of the Bcl-2 family [28,29]. Increased levels of Bax proteins have been reported to directly induce the release of cytochrome *c* by forming a pore in the outer membrane of the mitochondria [30]. Recently it has been shown that cytosolic p53 inhibits anti-apoptotic Bcl-xL and promotes cytochrome *c* release. Another study has demonstrated that p53 can directly modulate Bax-oligomerization, thereby priming cells for apoptosis by destabilizing the mitochondria [31,32]. In the present study, treatment of HeLa cells with azadirachtin and nimbolide resulted in an increase in the expression of Bax and Bid with concomitant decrease in the expression of Bcl-2 and Bcl-xL. It is conceivable that the Bcl-2 family proteins participate in the events that control the mitochondrial transmembrane potential in a p53-dependent manner triggering the release of cytochrome *c* during apoptosis induced by azadirachtin and nimbolide. In a previous study, we demonstrated a key role for ROS and Bcl-2/Bax in apoptosis induced by nimbolide in human choriocarcinoma (BeWo) cells [23]. Taken together, these data provide compelling evidence that the neem limonoids azadirachtin and nimbolide transduce apoptosis by the mitochondrial pathway.

Inhibition of survivin, a member of the IAP family of proteins, and NF-κB activation may be important mechanisms by which azadirachtin and nimbolide

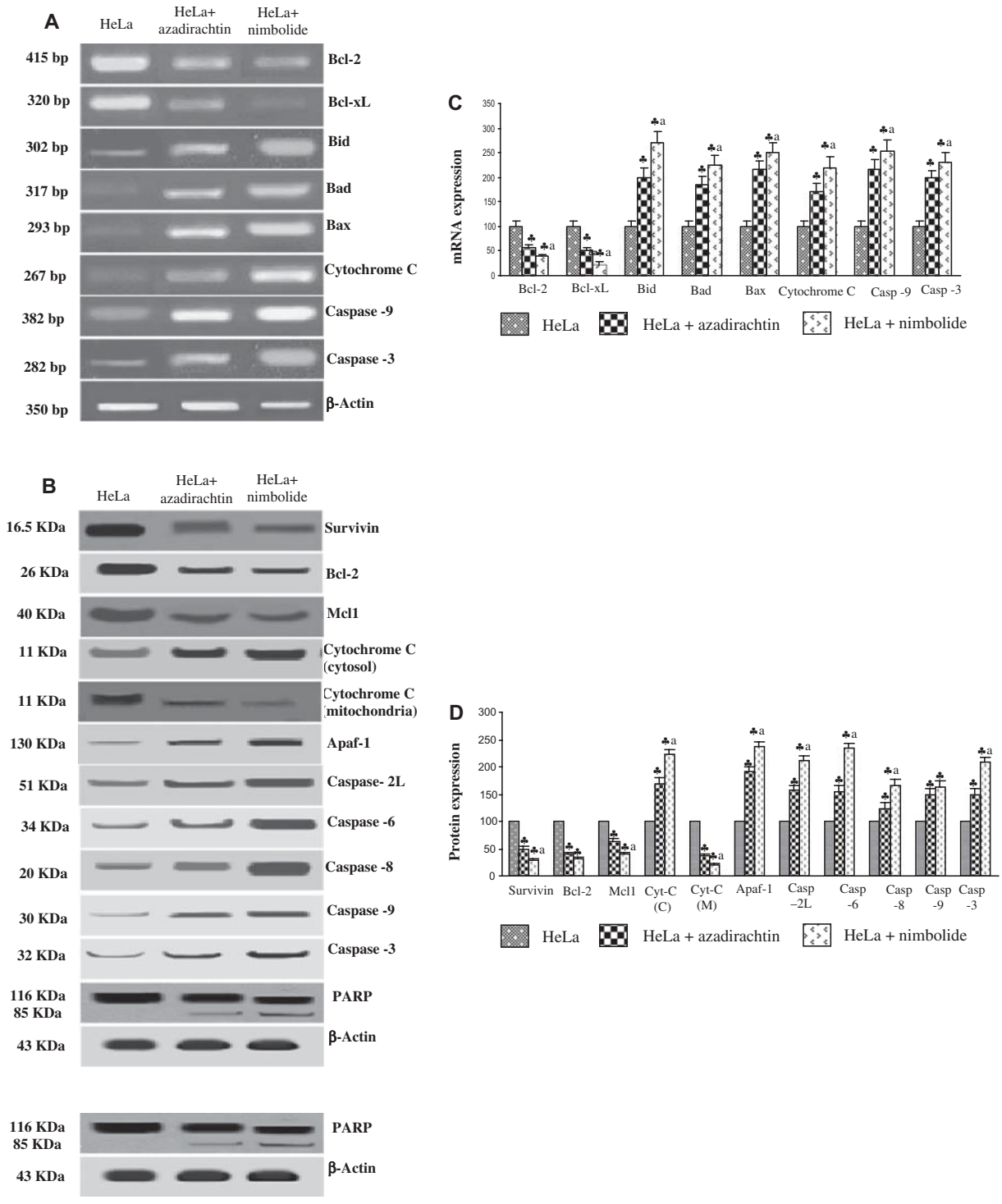

Figure 9. The effects of azadirachtin (135μM) and nimbolide (5μM) on markers of intrinsic apoptosis in HeLa cells. (A) Representative RT-PCR analyses. β-Actin was used as an internal control. (B) Representative immunoblots. Protein samples (50 μg/lane) resolved on SDS PAGE were probed with corresponding antibodies. β-Actin was used as loading control. (C, D) Densitometric analysis. ♣Significantly different from HeLa ($p<0.01$) ANOVA followed by LSD. 'a' Significantly different from HeLa+ Azadirachtin ($p<0.05$).

mediate mitochondrial apoptosis in HeLa cells. Survivin, a potent caspase inhibitor, blocks release of Smac/DIABLO from the mitochondria, whereas NF-κB activates anti-apoptotic proteins such as Bcl-xL and IAPs in addition to controlling the expression of cell cycle proteins such as cyclins, p21, p53 and PCNA [33,34]. Of late, both survivin and NF-κB have emerged as important targets for chemotherapy. Identification of potent inhibitors of survivin and NF-κB activation are therefore central in designing effective anti-cancer agents for therapy [35,36].

In conclusion, the results of the present study reveal that azadirachtin and nimbolide markedly

inhibit the growth of HeLa cells by inducing cell cycle arrest at G0/G1 phase and promoting the mitochondrial pathway of apoptosis. The greater efficacy of nimbolide relative to azadirachtin may be attributed to its *α,β*-unsaturated ketone element. Concerted modulation of cell cycle and apoptosis regulators is a major consideration in the search for novel anti-cancer drugs [37,38]. In particular, mitochondrial targeting is recognized to make tumour cells more susceptible to anti-cancer treatment [39]. However, a major obstacle in treatment targeted against individual molecules is the propensity for malignant tumours to switch to alternate pathways to evade apoptosis. Anti-oxidants such as azadirachtin and nimbolide that can simultaneously arrest the cell cycle and target multiple molecules involved in mitochondrial apoptosis offer immense potential as anti-cancer therapeutic drugs. Furthermore, the efficacy of these neem limonoids to inhibit chemically induced carcinogenesis *in vivo* at minimal concentration strengthens its therapeutic value [15,16]. Thus, the development of mechanism-based multi-targeted therapeutic strategies by natural products that display structural complexity, inherent biologic activity, affordability and lack of substantial toxic effects would help in rational design of drugs for cancer therapeutics.

Declaration of interest: This work was supported by a grant from the Department of Science and Technology, New Delhi, India. The authors report no conflicts of interest. The authors alone are responsible for the content and writing of the paper.

References

[1] Plati J, Bucur O, Khosravi-Far R. Dysregulation of apoptotic signaling in cancer: molecular mechanisms and therapeutic opportunities. J Cell Biochem 2008;104:1124–1149.
[2] Burz C, Berindan-Neagoe I, Balacescu O, Irimie A. Apoptosis in cancer: key molecular signaling pathways and therapy targets. Acta Oncol 2008;9:1–11.
[3] Schultz DR Jr, Harrington WJ. Apoptosis: programmed cell death at a molecular level. Semin Arthritis Rheum 2003;32: 345–369.
[4] Tan ML, Ooi JP, Ismail N, Moad AI, Muhammad TS. Programmed cell death pathways and current antitumor targets. Pharm Res 2009;26:1547–1560.
[5] Wallach D, Kang TB, Kovalenko A. The extrinsic cell death pathway and the élan mortel. Cell Death Differ 2008;15: 1533–1541.
[6] Logue SE, Martin SJ. Caspase activation cascades in apoptosis. Biochem Soc Trans 2008;36:1–9.
[7] Danial NN. Bcl-2 family proteins: critical checkpoints of apoptotic cell death. Clin Cancer Res 2007;13:7254–7263.
[8] Sethi G, Sung B, Aggarwal BB. Nuclear factor-κB activation: from bench to bedside. Exp Biol Med 2008;233:21–31.
[9] Salvesen GS, Duckett CS. IAP proteins: blocking the road to death's door. Nat Rev Mol Cell Biol 2002;3:401–410.
[10] Deorukhkar A, Krishnan S, Sethi G, Aggarwal BB. Back to basics: how natural products can provide the basis for new therapeutics. Expert Opin Investig Drugs 2007;16:1753–1773.
[11] Setzer WN, Setzer MC. Plant-derived triterpenoids as potential antineoplastic agents. Mini Rev Med Chem 2003;3:540–556.
[12] Akudugu J, Gäde G, Böhm L. Cytotoxicity of azadirachtin A in human glioblastoma cell lines. Life Sci 2001;68: 1153–1160.
[13] Cohen E, Quistad GB, Casida JE. Cytotoxicity of nimbolide, epoxyazadiradione and other limonoids from neem insecticide. Life Sci 1996;58:1075–1081.
[14] Roy MK, Kobori M, Takenaka M, Nakahara, Shinmoto H, Isobe S, Tsushida T. Antiproliferative effect on human cancer cell lines after treatment with nimbolide extracted from an edible part of the neem tree (Azadirachta indica). Phytother Res 2007;21:245–250.
[15] Priyadarsini RV, Manikandan P, Kumar GH, Nagini S. The neem limonoids azadirachtin and nimbolide inhibit hamster cheek pouch carcinogenesis by modulating xenobiotic-metabolizing enzymes, DNA damage, antioxidants, invasion and angiogenesis. Free Radic Res 2009;43:492–504.
[16] Harish Kumar G, Vidya Priyadarsini R, Vinothini G, Vidjaya Letchoumy P, Nagini S. The neem limonoids azadirachtin and nimbolide inhibit cell proliferation and induce apoptosis in an animal model of oral oncogenesis. Invest New Drugs 2009; [ePub 21 May 2009].
[17] Wang IK, Lin-Shiau SY, Lin JK. Induction of apoptosis by apigenin and related flavanoids through cytochrome C release and activation of caspase -9 and caspase -3 in leukaemia HL-60 cells. Eur J Cancer 1999;35:1517–1525.
[18] Smiley ST, Reers M, Mollola-Hartsorn C, Lin M, Chen A, Smith TW, Steele GD, Chen LB. Intracellular heterogeneity in mitochondrial membrane potentials revealed by a J-aggregate-forming lipophilic cation JC-1. Proc Natl Acad Sci USA 1991;88:3671–3675.
[19] Bradford MM. A rapid and sensitive method for the quantitation of microgram quantities of protein utilizing the principle of protein-dye binding. Anal Biochem 1976;72:248–254.
[20] Enari M, Sakahira H, Yokoyama H, Okawa K. A caspase activated DNase that degrades DNA during apoptosis and its inhibitor ICAD. Nature 1998;380:723–726.
[21] Clerkin JS, Naughton R, Quiney C, Cotter TG. Mechanisms of ROS modulated cell survival during carcinogenesis. Cancer Lett 2008;266:30–36.
[22] Roy MK, Kobori M, Takenaka M, Nakahara K, Shinmoto H, Tsushida T. Inhibition of colon cancer (HT-29) cell proliferation by a triterpenoid isolated from Azadirachta indica is accompanied by cell cycle arrest and up-regulation of p21. Planta Med 2006;72:917–923.
[23] Harish Kumar G, Chandra Mohan KVP, Jagannadha Rao A, Nagini S. Nimbolide a limonoid from Azadirachta indica inhibits proliferation and induces apoptosis of human choriocarcinoma (BeWo) cells. Invest New Drugs 2009;27:236–252.
[24] Thayyullathil F, Chathoth S, Hago A, Patel M, Galadari S. Rapid reactive oxygen species (ROS) induced by curcumin leads to caspase-dependent and independent apoptosis in L929 cells. Free Radic Biol Med 2008;45:1403–1412.
[25] Madan E, Prasad S, Roy P, George J, Shukla Y. Regulation of apoptosis by resveratrol through JAK/STAT and mitochondria mediation pathway in human epidermoid carcinoma A431 cells. Biochem Biophys Res Commun 2008;377: 1232–1237.
[26] Mohan KV, Gunasekaran P, Varalakshmi E, Hara Y, Nagini S. *In vitro* evaluation of the anticancer effect of lactoferrin and tea polyphenol combination on oral carcinoma cells. Cell Biol Int 2007;31:599–608.
[27] Boots AW, Haenen GR, Bast A. Health effects of quercetin: from antioxidant to nutraceutical. Eur J Pharmacol 2008; 585:325–337.
[28] Youle RJ, Strasser A. The Bcl-2 protein family: opposing activities that mediate cell death. Nat Rev Mol Cell Biol 2008;9:47–59.

[29] Brunelle JK, Letai A. Control of mitochondrial apoptosis by the Bcl2 family proteins. J Cell Sci 2009;122:437–441.
[30] Costantini P, Jacotot E, Decaudin D, Kroemer G. Mitochondrion as a novel target of anticancer chemotherapy. J Natl Cancer Inst 2000;92:1042–1053.
[31] Mihara M, Erster S, Zaika A, Petrenko O, Chittenden T, Pancoska P, Moll UM. p53 has a direct apoptogenic role at the mitochondria. Mol Cell 2003;11:552–554.
[32] Chipuk JE, Kuwana T, Bouchier-Hayes L, Droin NM, Newmeyer DD, Schuler M, Green DR. Direct activation of Bax by p53 mediates mitochondrial membrane permeabilization and apoptosis. Science 2004;303:1010–1014.
[33] Sah NK, Khan Z, Khan GJ, Bisen PS. Structural, functional and therapeutic biology of survivin. Cancer Lett 2006;244: 164–171.
[34] Pacifico F, Leonardi A. NF-kappaB in solid tumors. Biochem Pharmacol 2006;72:1142–1152.
[35] Ryan BM, O'Donovan N, Duffy MJ. Survivin: a new target for anti-cancer therapy. Cancer Treat Rev 2009;35:553–562.
[36] Shen HM, Tergaonkar V. NFkappaB signaling in carcinogenesis and as a potential molecular target for cancer therapy. Apoptosis 2009;14:348–363.
[37] Meeran SM, Katiyar SK. Cell cycle control as a basis for cancer chemoprevention through dietary agents. Front Sci 2008;13:2191–2202.
[38] Mac Farlane M. Cell death pathways- potential therapeutic target. Xenobiotica 2009;39:616–624.
[39] Gogvadze V, Orrenius S, Zhivotovsky B. Mitochondria as targets for cancer chemotherapy. Semin Cancer Biol 2009;19:57–66.

This paper was first published online on Early Online on 27 April 2010.